International Journal of Power Electronics and Drive System (IJPEDS)
Vol. 17, No. 4, December 2026, pp. 2495~2503
ISSN: 2088-8694, DOI: 10.11591/ijpeds.v17.i4.pp2495-2503

Modified DC–DC converter for BLDC motor drives: Technical overview and commutation torque ripple reduction

Sunam Saha[1], Madhurima Chattopadhyay[2], Moumita Mukherjee[1]
[1]Department of Electrical and Electronics Engineering, School of Engineering and Technology, Adamas University, Kolkata, India
[2]Heritage Institute of Technology, Kolkata, India

Article Info

Article history:

Received Mar 27, 2026
Revised Aug 31, 2026
Accepted Oct 4, 2026

Keywords:

BLDC drive
Brushless DC motor
DC-DC converter
Review
Torque ripple

ABSTRACT

Brushless DC motors (BLDCMs) have emerged as a preferred alternative to conventional motors across a wide range of applications, including household appliances, industrial systems, and electric vehicles. Their growing adoption stems not only from strong performance in position and speed regulation, but also from advantages such as high-power density, low-noise operation, and compatibility with electronic control. However, a persistent challenge in BLDC drives is torque ripple, which remains a key limitation of the technology. This paper presents a concise review of the different factors contributing to torque ripple in BLDCMs. Since reducing torque ripple is essential for achieving energy-efficient operation in BLDC drives, this work proposes a novel switched-capacitor-based ZETA hybrid converter as a means of suppressing it. In addition, the paper surveys various modified converter topologies currently used for this purpose. Findings indicate that the drive achieves minimal torque ripple at a specific converter duty ratio, and that both the ripple magnitude and commutation time vary as the duty ratio is adjusted.

This is an open access article under the CC BY-SA license.

Corresponding Author:

Sunam Saha
Department of Electrical and Electronics Engineering, School of Engineering and Technology
Adamas University
Kolkata 700126, India
Email: sunamsaha.ee@gmail.com

1. INTRODUCTION

Brushless DC motors (BLDCM) have become an attractive choice for industrial and domestic applications owing to their wide speed range, simple structure, noiseless operation, and ease of electronic control [1], [2]. BLDCM operation relies on sensing the rotor position to determine the voltage required to drive the motor, and this is achieved through two broad approaches. The Hall-effect sensor-based method uses physical sensors to obtain rotor position relative to the stator, while the sensorless approach estimates the back electromotive force (back-EMF) to energize the correct phase at the correct instant [2]-[4]. Sensorless techniques combined with intelligent switching strategies, such as hybrid model predictive current control for six-step commutation, have recently been proposed to improve commutation accuracy without added hardware cost [5], [6].

In BLDCM, the motor controller plays an important role in operating and regulating the speed, position, and torque of the motor, enabling the user to start, stop, and control the motor at required specifications [3]-[5]. In the motor controller, the different motor operational parameters are used as input quantities to offer desired performance and ensure proper flow of energy in the motor. Developing a motor controller to regulate the motor drive system is a challenging task, which is achieved using advanced power electronics converters [6]-[9]. Different power converters are presented in the literature that offer different

advantages. A brief overview of the hybrid DC-DC converter is presented in section 3. BLDCM controllers are required to attain smooth torque and speed to ensure efficient motor operation. Due to different variations in parameters and uncertainties, smooth motor rotation is not achieved, and this leads to increases and decreases in torque, thus creating torque ripple [10]-[15]. The different causes of torque ripple are studied and presented in section 2 of this paper.

The major difficulty in BLDCM is the presence of torque ripple. A simple method to minimize torque ripple in a BLDCM drive is to implement a duty ratio control of the DC power converter [7]-[20]. Section 3 shows a review of different hybrid converters. Section 4 elaborates on a new hybrid converter for providing supply to the inverter and, in turn, minimizing the torque ripple. In this paper, an elaborate discussion on the causes of torque ripple in BLDCM and a review of different available hybrid converters is presented along with a new hybrid converter. Section 5 establishes a relation between converter DC output voltage, torque ripple, motor speed, and total harmonic distortion content in electromagnetic torque. The results obtained from the proposed drive are discussed in section 5, and lastly the concluding remarks are presented in section 6.

2. BRIEF REVIEW ON SOURCES OF RIPPLE IN BLDCM

The presence of torque ripple is one of the key factors limiting the practical application of BLDC drives. Achieving high-performance operation requires smooth output torque, so understanding what generates ripple is essential. The sources of torque ripple can be broadly grouped into two categories: those arising from motor construction and those arising from motor operating and control parameters [9]-[15]. The classification is presented in Figure 1. Ripple magnitude depends on factors such as motor design, control strategy, and real-time operating conditions. Each contributing cause is discussed below.

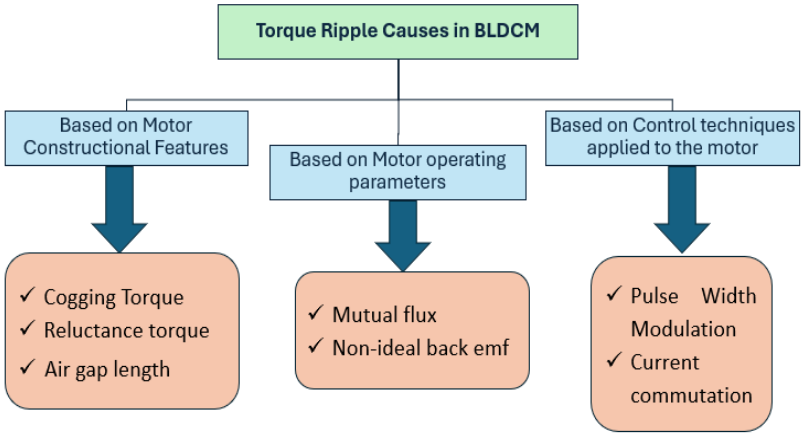

Figure 1. Sources of ripple in BLDC

2.1. Based on motor construction

2.1.1. Cogging torque

Cogging torque arises from the magnetic interaction between the rotor's permanent magnets and the stator teeth. As the magnetic field intensity varies with rotor position, the resulting attraction force becomes non-uniform, producing unequal torque and hence ripple. Slot width, skewing, and magnet width all influence the severity of cogging torque [4], [7], [8]. It can be reduced at the design stage by increasing the number of slots per pole, widening the air gap, or narrowing the slot opening.

2.1.2. Reluctance torque

In a BLDC motor, the reluctance torque is a small component of torque generated due to variation in reluctance within the motor. This variation occurs due to a change in the position of the rotor [4]. The reluctance torque is influenced by the stator and rotor teeth geometry.

2.1.3. Air gap length

The design of BLDCM includes material selection and machine structure and sizing of the geometry of the different components of the machine. One of the important components is the air gap length selection, which is obtained by considering the mechanical, thermal, and electromagnetic factors of the machine. The air gap length is an essential element that influences the magnetic circuit and efficiency of the motor. The electromagnetic torque in BLDCM depends upon the back EMF, and the air gap length influences the flux density, which in turn changes the flux linkage and back EMF of the machine [4], [13].

2.2. Based on motor operating parameters

2.2.1. Mutual flux

In a BLDC motor, mutual flux is the flux linkage shared between two stator phases of the BLDC motor. The motor performance can be improved by reducing the leakage flux. The leakage flux can be influenced by the design and construction of the stator parameters of the motor [7].

2.2.2. Non-ideal back EMF

Ideally, a BLDC motor drive is expected to provide a rectangular current wave shape in phase with the trapezoidal back EMF by controlling the switching of the inverter connected to the stator of the BLDC motor. However, the non-ideal nature of the power converter and the inductance of the stator winding make the current deviate from the rectangular wave shape. This deviation, in turn, increases the torque ripple [8].

2.3. Based on motor operating parameters

2.3.1. Pulse width modulation

Pulse width modulation is a technique used to vary the width of a voltage pulse, which in turn is utilized to control the switching or output voltage magnitude in a power modulator. In a BLDC motor, PWM is applied to modulate the duty ratio in a converter circuit. It may also be applied to inverter switches to minimize torque ripple [4], [9].

2.3.2. Current commutation

For operation of a BLDC motor, the inverter used is mostly operated in 120-degree mode of operation along with three Hall sensors for determining the rotor position and requires trapezoidal back EMF. During the operation, the current phase changes; as a result, the current is commutated from one phase to another. This transient operation in current leads to ripple in torque called commutation torque ripple. To reduce the commutation torque ripple, different methods are proposed, including computation of commutation time and modulating duty ratio to reduce torque ripple [8]-[13].

3. REVIEW ON HYBRID BOOST CONVERTERS

DC-DC converters increase voltage gain in BLDCM drives [14]. Boost converters are broadly isolated (transformer-based, gain set by turns ratio [15]) or non-isolated. Transformer-based isolation raises leakage inductance, voltage stress, and losses, so non-isolated converters, simpler and more compact, are generally preferred [18]. However, conventional non-isolated converters cannot reach high gain at very high duty ratios [20], so hybrid networks of inductors, capacitors, diodes, and switches are used instead. These fall into four families: inductor-inductor, inductor-capacitor, capacitor-capacitor, and hybrid, reviewed below. Common design principles include: parallel charging/series discharging of storage elements for higher gain; supplying the load jointly from the source and capacitor during switch-off; replacing diodes with inductors; and adding capacitors that loop with the diode, switch, and load to cut voltage stress.

3.1. Inductor-inductor topology

Two inductors store and release energy, giving rise to switched-inductor, interleaved, switched-inductor-with-capacitor, and quadratic boost variants. Switched-inductor designs [21]-[24] raise gain (up to ~10×) at low duty ratio with simple control, but increase input current ripple, limiting use where low ripple is needed. Interleaved designs [25]-[27] use alternately energized inductors to lower current ripple and enable step-up/step-down or multi-phase operation, but gain stays moderate, and more switches raise control complexity and cost. Switched-inductor-with-capacitor [28] boosts gain further, but risks inrush current at the source during switch-off. Quadratic boost converters [29]-[31] roughly square the gain of a conventional boost stage while offering continuous input current and common grounding, reducing EMI and ripple, making this one of the more attractive options for high-gain applications.

3.2. Capacitor-capacitor topology

Two capacitors combine into switched-capacitor, voltage-multiplier, or Z-source structures. Switched-capacitor (SC) designs [32]-[34] achieve high gain and good transient response but lack common grounding and retain output ripple, with harder control than switched-inductor designs. Voltage multipliers (Cockcroft-Walton, Dickson, single-stage) [35] have been combined with interleaved and classical boost stages to match renewable-energy bus voltages, at the cost of more stages, component count, and switching stress. Z-source converters [32]-[34] achieve high gain at low duty ratio, with later variants offering common grounding and lower-cost MOSFETs, but suffer from pulsating output current.

3.3. Inductor-capacitor topology

Inductor-capacitor voltage-lift circuits originated with Luo's super-lift converters [33]. They have been extended to quadratic and standard boost converters [21]-[23] to achieve higher gain with fewer switches and lower stress. Duty-ratio selection is critical, while pulsating current remains the main limitation.

3.4. Hybrid converter topology

Hybrid designs combine multiple elements, including interleaved converters with voltage multipliers, CUK-boost combinations, SEPIC with voltage multipliers, and Z-source/switched-inductor-capacitor combinations [30]. The latter can achieve a voltage gain of up to 21× using a single switch. Trade-offs between gain, component count, and stress differ across designs, motivating continued research toward an all-around optimal topology.

4. PROPOSED METHOD TO MINIMIZE TORQUE RIPPLE

The previous section presented different design possibilities of a hybrid converter. For this work, a new hybrid converter with switched capacitor-based technology is implemented in the ZETA converter. This modified ZETA converter is incorporated as a power modulator in a BLDCM drive to minimize torque ripple. The choice is based on the advantages of the ZETA converter in reducing total harmonic distortion in the BLDCM drive and the voltage gain obtained from the switched capacitor structure. The circuit diagram of the proposed hybrid converter for BLDC drive is presented in Figure 2.

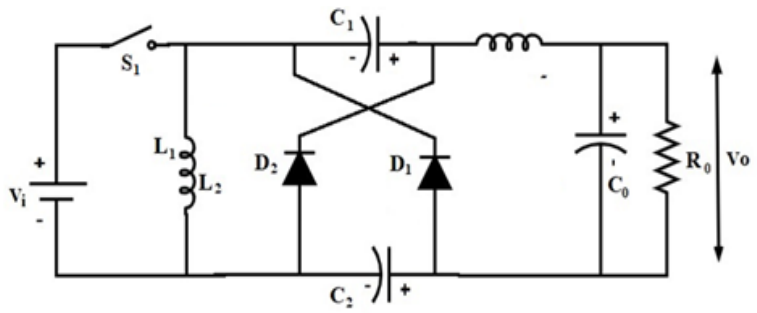

Figure 2. Circuit diagram of hybrid boost converter

The hybrid converter with a switched capacitor is placed as an input DC source for the inverter to operate the BLDCM. The block diagram representation of the BLDCM drive circuit is presented in Figure 3. The simulation for the proposed drive is shown in Figure 4. The electromagnetic torque obtained from the torque output is analyzed for torque ripple and total harmonic distortion with changes in the duty cycle of the DC power modulator with a switched capacitor. The obtained results are discussed in the results and discussion.

Another parameter that affects the commutation torque ripple is the motor speed. Back EMF is proportional to the speed and is considered constant during commutation. The commutation torque ripple spikes at low speeds and dips in the high-speed range. Depending on the rise time, fall time, and the speed of the motor, three different states of operation are possible during operation of the motor. The three states of phase current conditions are presented in Figure 5. In Figure 5(a), Vdc > 4 E, then tf > tr, and the torque spikes during commutation. In Figure 5(b), Vdc < 4 E, then tf < tr, and the torque dips during commutation. In Figure 5(c), Vdc = 4 E, then tf = tr, and the torque remains constant during commutation.

From the above three cases, we may say that by modulating Vdc, the torque ripple can be modulated. Therefore, a DC-DC converter is used to provide a controlled DC input to the inverter.

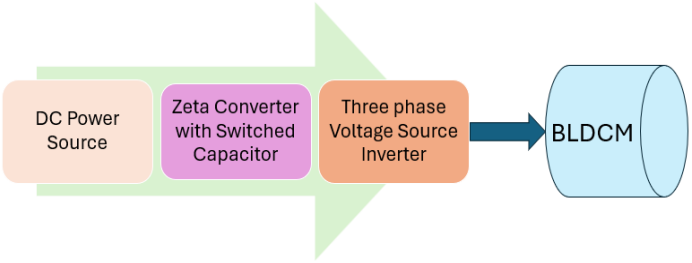

Figure 3. Block diagram of proposed BLDC drive

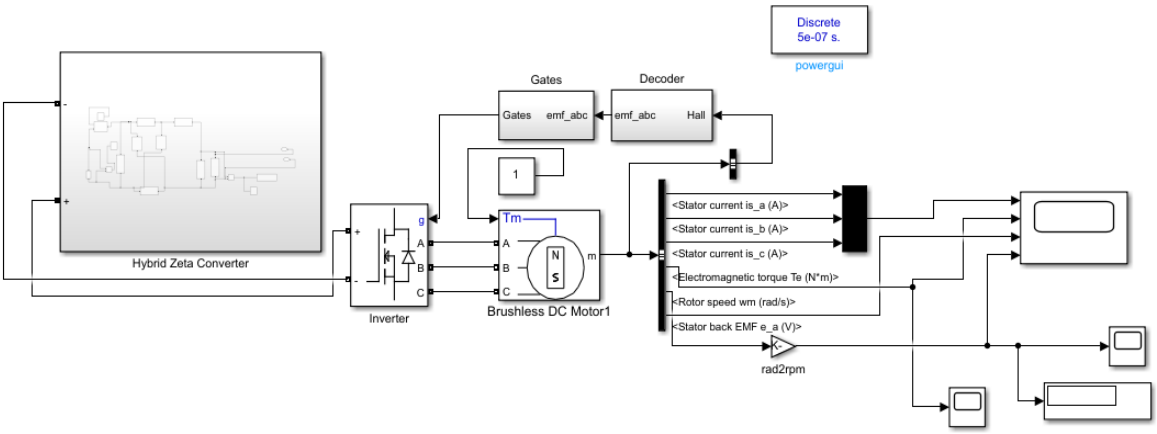

Figure 4. Simulation diagram of proposed BLDC drive

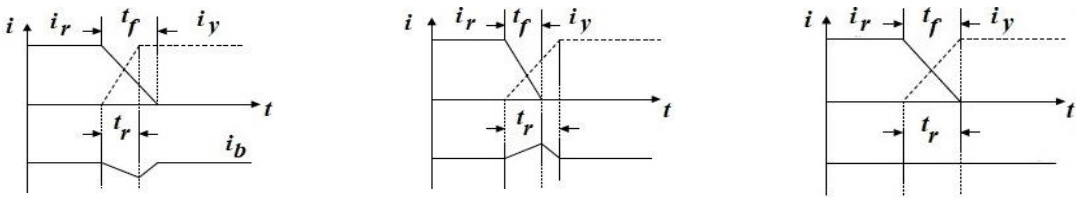

Figure 5. Phase current behavior during commutation

5. RESULTS AND DISCUSSION

The switched-capacitor-based ZETA converter was configured using parameters presented in Table 1. The converter's output DC voltage was used to feed the six-step inverter driving the BLDCM. The duty cycle (D) of the converter's switching signal was varied from 60% to 90% in 5% steps, and for each value of D the following quantities were recorded at steady state: stator phase current, electromagnetic torque, stator back-EMF, rotor speed, commutation time, torque ripple percentage, and THD of the electromagnetic torque.

The torque ripple computed over one electrical cycle at steady state is calculated as: Torque ripple (%) = [(T_max − T_min) / T_avg] × 100. Commutation time is the interval measured between the start of the current transition following a Hall-sensor edge and the current in the incoming phase reaching its steady value. THD (%) is computed via FFT of the electromagnetic torque waveform.

Table 1. Converter design parameters for the proposed drive

Parameter	Value
Input DC voltage	30 V
Switching frequency	100 kHz
Inductor L_1	500 µH
Inductor L_2	2000 µH
Capacitors C_1, C_2, C_3	5 µF each
Load resistance	30 Ω
Load torque (constant)	1 Nm

The switched capacitor-based ZETA converter offered very high gain. The power modulator is operated at 100 kHz frequency for a 30 Volt input. It comprises two inductor coils of 500 µH and 2000 µH, three capacitors of 5 µF each, and a resistive load of 30 Ω. The output DC voltage obtained is provided as input for the inverter, which is operating the BLDCM of the proposed drive. The load torque is maintained constant during the entire operation at 1 Nm. The ripple content in the output torque of the BLDCM is calculated for the change in duty cycle of the DC power modulator. The stator phase current, electromagnetic torque, stator back-EMF, and rotor speed obtained are depicted in Figure 6. Along with torque ripple, the current commutation time is noted and tabulated with the change in duty ratio. The data obtained are presented in Table 2.

Table 2. Variation of drive parameters with duty cycle

Duty cycle	Mean torque	Commutation time (µ sec)	Torque ripple %	Motor speed	THD%
90	1.35	132.92	59.29	1528	85.88
85	1.153	79.89	59.67	1437	70.7
80	1.1234	135.43	57.33	1217	56.9
75	1.105	173.66	53.66	1002	42.94
70	1.096	411.4	30.93	820.8	24.35
65	1.068	137.22	52.72	673.5	26.7
60	1.58	232.49	32.53	554	32.56

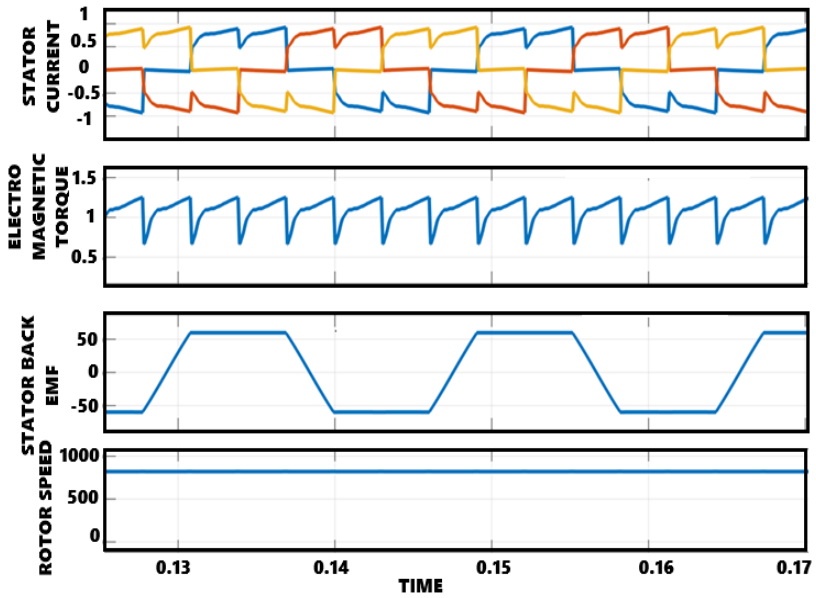

Figure 6. BLDC drive output

As duty cycle increases from 60% to 90%, the converter's output DC-link voltage rises, and this is directly reflected in rotor speed: motor speed increases nearly monotonically from 554 rpm at D = 60% to 1528 rpm at D = 90%. This behavior is consistent with the fundamental BLDCM speed relationship: rotor speed scales with the applied DC-link voltage (via back-EMF) at a fixed load torque of 1 Nm. This confirms that the switched-capacitor ZETA converter is functioning as intended: duty cycle is an effective handle for continuously varying the inverter's supply voltage and, consequently, motor speed.

Torque ripple does not track speed monotonically. Starting from D = 90% (59.29% ripple), ripple decreases steadily as duty cycle is reduced: 59.67% (D=85%), 57.33% (D=80%), 53.66% (D=75%), reaching a clear minimum of 30.93% at D = 70%. Below this point, ripple rises sharply again to 52.72% at D = 65% before settling near 32.53% at D = 60%. This change is represented in Figure 7. This non-monotonic, U-shaped trend indicates that torque ripple is minimized at a specific optimal DC-link voltage rather than simply improving as voltage is reduced. At high duty cycles, the elevated DC-link voltage likely overdrives the commutating phase current, producing steeper current transitions and larger ripple spikes at each commutation instant. At low duty cycles, insufficient DC-link voltage appears to slow the commutation process, leaving current transitions incomplete before the next commutation event and reintroducing ripple. The 70% duty cycle represents the point at which the DC-link voltage is best matched to the motor's back-EMF and winding dynamics, allowing current commutation to complete cleanly within each conduction interval.

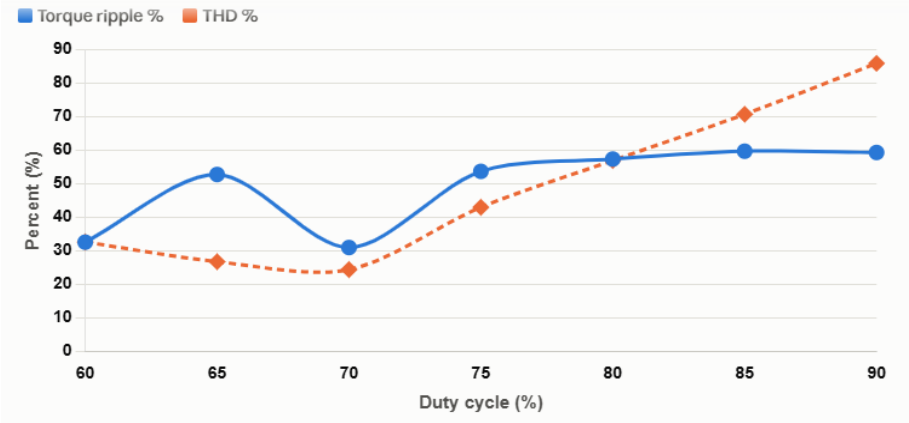

Figure 7. Graphical representation of the change in torque ripple and THD with duty ratio

6. CONCLUSION

This paper examined torque ripple in BLDC motor drives, its origins, mitigation approaches, and an experimental case study. Torque ripple sources were classified into motor-construction factors (cogging torque, reluctance torque, air-gap-dependent flux variation) and operating/control factors (mutual flux, non-ideal back-EMF, PWM, current commutation), showing that effective mitigation depends on correctly identifying the dominant source in a given drive. A review of non-isolated hybrid DC-DC converters, spanning inductor-inductor, capacitor-capacitor, inductor-capacitor, and hybrid topologies, confirmed that duty-ratio-controlled DC-link regulation remains one of the most practical, hardware-light strategies for suppressing torque ripple, since no single topology optimizes gain, component count, and voltage stress simultaneously.

Experimental results using a switched-capacitor-based ZETA converter validated this approach directly. Sweeping the duty cycle from 60% to 90% showed that while motor speed scales predictably with duty cycle, torque ripple and THD follow a U-shaped trend, both reaching a simultaneous minimum of 30.93% ripple and 24.35% THD at 70% duty cycle. This optimum coincided with the longest recorded commutation interval (411.4 µs), indicating that ripple suppression is driven by smoother, more gradual current commutation rather than faster switching. These findings confirm that regulating DC-link voltage via converter duty ratio can substantially reduce torque ripple without added sensors or control complexity, using a compact converter design. Future work will derive the converter's complete state-space model to analytically predict the optimal duty ratio for arbitrary motor and load conditions, and extend this analysis to variable-load and variable-speed operation.

FUNDING INFORMATION

Authors state no funding involved.

AUTHOR CONTRIBUTIONS STATEMENT

This journal uses the Contributor Roles Taxonomy (CRediT) to recognize individual author contributions, reduce authorship disputes, and facilitate collaboration.

Name of Author	C	M	So	Va	Fo	I	R	D	O	E	Vi	Su	P	Fu
Sunam Saha	✓	✓	✓	✓	✓	✓	✓	✓	✓	✓			✓	
Madhurima Chattopadhyay		✓				✓				✓	✓	✓		
Moumita Mukherjee	✓		✓	✓			✓			✓	✓	✓		

C : **C**onceptualization
M : **M**ethodology
So : **So**ftware
Va : **Va**lidation
Fo : **Fo**rmal analysis
I : **I**nvestigation
R : **R**esources
D : **D**ata Curation
O : Writing - **O**riginal Draft
E : Writing - Review & **E**diting
Vi : **Vi**sualization
Su : **Su**pervision
P : **P**roject administration
Fu : **Fu**nding acquisition

CONFLICT OF INTEREST STATEMENT

Authors state no conflict of interest.

DATA AVAILABILITY

Data availability is not applicable to this paper as no new data were created or analyzed in this study.

REFERENCES

[1] S. Saha, D. Chowdhury, M. Chattopadhyay, and M. Mukherjee, "A novel technique for torque ripple suppression in BLDC motor drive using switched capacitor based SEPIC converter," *International Journal of Power Electronics and Drive Systems (IJPEDS)*, vol. 15, no. 1, Mar. 2024, doi: 10.11591/ijpeds.v15.i1.pp27-34.

[2] Z. Chen, J. Qi, X. Chen, J. Xu, Y. Liu, and Z. Dong, "Parallel converter cell-based step-down bridgeless PFC converters with wide output for BLDC motor," *IEEE Transactions on Industry Applications*, vol. 61, no. 2, pp. 3293–3302, 2025, doi: 10.1109/TIA.2025.3531820.

[3] P. Pillay and R. Krishnan, "Modeling, simulation, and analysis of permanent-magnet motor drives. II. The brushless DC motor drive," *IEEE Transactions on Industry Applications*, vol. 25, no. 2, pp. 274–279, 1989, doi: 10.1109/28.25542.

[4] N. Prabhu, R. Thirumalaivasan, and B. Ashok, "Critical review on torque ripple sources and mitigation control strategies of BLDC motors in electric vehicle applications," *IEEE Access*, vol. 11, pp. 115699–115739, 2023, doi: 10.1109/ACCESS.2023.3324419.

[5] R. Çelikel and Ö. Aydogmus, "A torque ripple minimization method for brushless dc motor in high speed applications using buck boost topology," *Journal of Engineering Research (Kuwait)*, vol. 7, no. 3, pp. 200–214, 2019, doi: 10.1016/s2307-1877(25)00612-1.

[6] R. A. and A. Gnana Saravanan, "Torque ripple minimization of bridgeless CUK converter-based BLDC motor using improved jellyfish search algorithm," *ISA Transactions*, vol. 136, pp. 374–389, May 2023, doi: 10.1016/j.isatra.2022.11.025.

[7] M. Sumega, Š. Zoššák, P. Varecha, and P. Rafajdus, "Sources of torque ripple and their influence in BLDC motor drives," *Transportation Research Procedia*, vol. 40, pp. 519–526, 2019, doi: 10.1016/j.trpro.2019.07.075.

[8] J.-H. Song and I. Choy, "Commutation torque ripple reduction in brushless DC motor drives using a single DC current sensor," *IEEE Transactions on Power Electronics*, vol. 19, no. 2, pp. 312–319, Mar. 2004, doi: 10.1109/TPEL.2003.823177.

[9] S. Mondal, A. Dey, S. Saha, and M. Chattopadhyay, "BLDC Motor Performance in Cuk and Sheppard-Taylor topologies," in *2025 4th OPJU International Technology Conference (OTCON) on Smart Computing for Innovation and Advancement in Industry 5.0*, IEEE, Apr. 2025, pp. 1–5, doi: 10.1109/OTCON65728.2025.11070891.

[10] R. Heidari and J.-W. Ahn, "Torque ripple reduction of BLDC motor with a low-cost fast-response direct DC-Link current control," *IEEE Transactions on Industrial Electronics*, vol. 71, no. 1, pp. 150–159, Jan. 2024, doi: 10.1109/TIE.2023.3247732.

[11] J. Hu, D. Yang, and Z. Sun, "Torque fluctuation suppression strategy of integrated electric drive system based on the principle of minimization of instantaneous current tracking error," *IEEE Access*, vol. 10, pp. 124673–124684, 2022, doi: 10.1109/ACCESS.2022.3225103.

[12] Z. Li, Q. Kong, S. Cheng, and J. Liu, "Torque ripple suppression of brushless DC motor drives using an alternating two-phase and three-phase conduction mode," *IET Power Electronics*, vol. 13, no. 8, pp. 1622–1629, Jun. 2020, doi: 10.1049/iet-pel.2019.0960.

[13] W. Jiang, Y. Liao, J. Wang, P. Wang, and Y. Xie, "Improved control of BLDCM considering commutation torque ripple and commutation time in full speed range," *IEEE Transactions on Power Electronics*, vol. 33, no. 5, pp. 4249–4260, May 2018, doi: 10.1109/TPEL.2017.2717484.

[14] M. Forouzesh, Y. P. Siwakoti, S. A. Gorji, F. Blaabjerg, and B. Lehman, "A survey on voltage boosting techniques for step-up DC-DC converters," in *2016 IEEE Energy Conversion Congress and Exposition (ECCE)*, 2016, pp. 1–8, doi: 10.1109/ECCE.2016.7854792.

[15] B. Axelrod, Y. Berkovich, and A. Ioinovici, "Switched-capacitor/switched-inductor structures for getting transformerless hybrid DC–DC PWM converters," *IEEE Transactions on Circuits and Systems I: Regular Papers*, vol. 55, no. 2, pp. 687–696, Mar. 2008, doi: 10.1109/TCSI.2008.916403.

[16] Y. Tang, D. Fu, T. Wang, and Z. Xu, "Hybrid switched-inductor converters for high step-up conversion," *IEEE Transactions on Industrial Electronics*, vol. 62, no. 3, pp. 1480–1490, Mar. 2015, doi: 10.1109/TIE.2014.2364797.

[17] P. K. Maroti, S. Padmanaban, P. Wheeler, F. Blaabjerg, and M. Rivera, "Modified boost with switched inductor different configurational structures for DC-DC converter for renewable application," *Proceedings - 2017 IEEE Southern Power Electronics Conference, SPEC 2017*, vol. 2018-January, pp. 1–6, 2017, doi: 10.1109/SPEC.2017.8333674.

[18] J. Liu, D. Gao, and Y. Wang, "High power high voltage gain interleaved DC-DC boost converter application," *2015 6th International Conference on Power Electronics Systems and Applications: Electric Transportation - Automotive, Vessel and Aircraft, PESA 2015*, 2016, doi: 10.1109/PESA.2015.7398903.

[19] D. Gao, Z. Jin, J. Liu, and M. Ouyang, "An interleaved step-up/step-down converter for fuel cell vehicle applications," *International Journal of Hydrogen Energy*, vol. 41, no. 47, pp. 22422–22432, 2016, doi: 10.1016/j.ijhydene.2016.09.171.

[20] M. A. Salvador, T. B. Lazzarin, and R. F. Coelho, "High step-up DC–DC converter with active switched-inductor and passive switched-capacitor networks," *IEEE Transactions on Industrial Electronics*, vol. 65, no. 7, pp. 5644–5654, Jul. 2018, doi: 10.1109/TIE.2017.2782239.

[21] P. Yang, J. P. Xu, S. Y. Zhang, and F. Zhang, "Energy transmission mode of quadratic CCM Boost converter," *Dianji yu Kongzhi Xuebao/Electric Machines and Control*, vol. 16, no. 6, pp. 44–49, 2012.
[22] P. K. Maroti, S. Padmanaban, J. B. Holm-Nielsen, M. Sagar Bhaskar, M. Meraj, and A. Iqbal, "A new structure of high voltage gain SEPIC converter for renewable energy applications," *IEEE Access*, vol. 7, pp. 89857–89868, 2019, doi: 10.1109/ACCESS.2019.2925564.
[23] M. Z. Malik, Q. Xu, A. Farooq, and G. Chen, "A new modified quadratic boost converter with high voltage gain," *IEICE Electronics Express*, vol. 14, no. 1, pp. 1–6, 2017, doi: 10.1587/elex.13.20161176.
[24] M. Veerachary and V. Khubchandani, "Analysis, design, and control of switching capacitor based buck–boost converter," *IEEE Transactions on Industry Applications*, vol. 55, no. 3, pp. 2845–2857, May 2019, doi: 10.1109/TIA.2018.2889848.
[25] S. Pirpoor, S. Rahimpour, M. Andi, N. Kanagaraj, S. Pirouzi, and A. H. Mohammed, "A novel and high-gain switched-capacitor and switched-inductor-based DC/DC boost converter with low input current ripple and mitigated voltage stresses," *IEEE Access*, vol. 10, pp. 32782–32802, 2022, doi: 10.1109/ACCESS.2022.3161576.
[26] M. Kumar, V. K. Yadav, and A. K. Verma, "Switched capacitor based high gain boost converter for renewable energy application," *IEEE Journal of Emerging and Selected Topics in Industrial Electronics*, vol. 4, no. 3, pp. 818–826, 2023, doi: 10.1109/JESTIE.2023.3262451.
[27] J. F. Dickson, "On-chip high-voltage generation in MNOS integrated circuits using an improved voltage multiplier technique," *IEEE Journal of Solid-State Circuits*, vol. 11, no. 3, pp. 374–378, Jun. 1976, doi: 10.1109/JSSC.1976.1050739.
[28] R. Saravanan and N. Jaya, "Multistage boost converter with modified voltage multiplier for contemporary applications," *Journal of Electrical Engineering and Technology*, vol. 19, no. 7, pp. 4323–4333, 2024, doi: 10.1007/s42835-024-01857-0.
[29] X. Fang, "A novel Z-source DC-DC converter," *Proceedings of the IEEE International Conference on Industrial Technology*, 2008, doi: 10.1109/ICIT.2008.4608314.
[30] H. Shen, B. Zhang, D. Qiu, and L. Zhou, "A common grounded Z-source DC-DC converter with high voltage gain," *IEEE Transactions on Industrial Electronics*, vol. 63, no. 5, pp. 2925–2935, 2016, doi: 10.1109/TIE.2016.2516505.
[31] S. Rostami, V. Abbasi, and T. Kerekes, "Switched capacitor based Z-source DC-DC converter," *IET Power Electronics*, vol. 12, no. 13, pp. 3582–3589, 2019, doi: 10.1049/iet-pel.2019.0633.
[32] Fang Lin Luo and Hong Ye, "Positive output super-lift converters," *IEEE Transactions on Power Electronics*, vol. 18, no. 1, pp. 105–113, Jan. 2003, doi: 10.1109/TPEL.2002.807198.
[33] F. Mohammadzadeh Shahir, E. Babaei, and M. Farsadi, "Voltage-lift technique based non isolated boost DC–DC converter: Analysis and design," *IEEE Transactions on Power Electronics*, vol. 33, no. 7, pp. 5917–5926, Jul. 2018, doi: 10.1109/TPEL.2017.2740843.
[34] A. Rajabi, A. Rajaei, V. M. Tehrani, P. Dehghanian, J. M. Guerrero, and B. Khan, "A non-isolated high step-Up DC-DC converter using voltage lift technique: analysis, design, and implementation," *IEEE Access*, vol. 10, pp. 6338–6347, 2022, doi: 10.1109/ACCESS.2022.3141088.
[35] M. Shaabani, A. Mirzaei, M. Rezvanyvardom, F. Khosravi, and S. A. Gorji, "A hybrid switched-inductor/switched-capacitor DC-DC converter with high voltage gain using a single switch for photovoltaic application," *Energies*, vol. 16, no. 14, Jul. 2023, doi: 10.3390/en16145524.

BIOGRAPHIES OF AUTHORS



Dr. Sunam Saha received her B.Tech. degree in electrical and electronics engineering in 2012 and her M.Tech. degree in power electronics in 2016 from Sikkim Manipal Institute of Technology, Sikkim, India. She received her Ph.D. degree from Adamas University, India, in 2024. With 10 years of teaching experience, she is currently an associate professor in the Department of Electrical Engineering at Adamas University. Her research interests include power electronic converters and electrical machines. She can be contacted at email: sunamsaha.ee@gmail.com.



Madhurima Chattopadhyay received her B.Tech. degree in instrumentation engineering from Jadavpur University and her M.Tech. degree in instrumentation engineering from the University of Calcutta, Kolkata, India. She also received her Ph.D. degree in instrumentation from the Indian Institute of Science, Bengaluru, India. She is currently a professor and head of the Department of Applied Electronics and Instrumentation Engineering at Heritage Institute of Technology, India. Her research interests include electrical machines, power converters, microsensors, and electrical impedance spectroscopy. She can be contacted at email: madhurima.chattopadhyay@heritageit.edu.



Moumita Mukherjee received her M.Sc. degree in applied physics from the University of Calcutta and her M.Tech. degree in biomedical engineering from the West Bengal University of Technology, India. She received her Ph.D. (Technology) degree through the University of Calcutta, based on her research at the Defence Research and Development Organisation (DRDO), India. She is currently a professor and Dean of Research and Development at Adamas University, India. She can be contacted at email: moumita.mukherjee@adamasuniversity.ac.in.